DALTON
FULL PAPER

Isolation, structural and spectroscopic investigations of complexes with tridentate [O,P,O] and [O,O,O] donor ligands

Rolf Siefert, Thomas Weyhermüller and Phalguni Chaudhuri *

Max-Planck-Institut für Strahlenchemie, Stiftstrasse 34-36, D-45470 Mülheim an der Ruhr, Germany. E-mail: Chaudh@mpi-muelheim.mpg.de

Received 14th July 2000, Accepted 16th October 2000
First published as an Advance Article on the web 28th November 2000

A phosphorus-containing potentially tridentate ligand bis(3,5-di-*tert*-butyl-2-hydroxyphenyl)phenylphosphine H_2L, **1**, was prepared. **1** reacts directly in solution with aerial oxygen or hydrogen peroxide to form bis(3,5-di-*tert*-butyl-2-hydroxyphenyl)phenylphosphine oxide H_2LO, **2**. It yields complexes $[Ni^{II}(HL)_2]$ **3**, $[Co^{III}(OH_2)(HL)(L)]$ **4**, $[Rh^{III}Cl(H_2L)(L)]$ **5**, and $[Rh^{III}(HL)(L)(H_2O)]$ **6** characterized by various physical techniques, including IR, MS, UV-vis, ^1H and ^{31}P-$\{^1H\}$ NMR and electrochemical methods. The crystal structures of **3**, **4** and **5** show tridentate [O,P,O] and bidentate [O,P,OH] coordination of deprotonated **1** and the coordination geometry of the metal centre. The structure of **2** reveals strong hydrogen bonding between the phenolic hydroxyl groups and the O=P group in the solid state. That the ligand **2** produces a weak ligand field providing tridentate [O,O,O] coordination sites has been evidenced by the structure and paramagnetism of $[Co^{II}_2(LO)_2(C_2H_5OH)_3]$ **7**.

Introduction

The current explosive development in the coordination chemistry of phenol-containing ligands[1] is mainly due to the discovery of the widespread occurrence of tyrosine radicals in metalloproteins involved in oxygen-dependent enzymatic radical catalysis.[2] Amongst the catalytically essential redox-active amino acids, tyrosine-based radical enzymes are the best characterized.

As part of an effort directed toward the development of biologically inspired homogeneous catalysts[3–5] for the aerial oxidation of organic substrates like alcohols, amines, *etc.*, we are investigating the synthesis and reactivity of phenolate complexes of the late transition metals, together with their one-electron oxidized phenoxyl-radical complexes. Such phenoxyl-radical complexes are rather rare. This is partly due to the fact that the metal–phenolate bond to a late-transition metal ion should be relatively weak. For the early transition metal ions the metal–phenolate bonding is strengthened by π donation from the lone pair of electrons on oxygen into an empty d orbital on the metal, but for the late transition metal ions such empty low-lying orbitals are not always available.

One of the major advantages of homogeneous catalysis is the possibility of fine tuning the catalyst by varying the ancillary ligands. In this way, chemo-, regio-, and stereo-selectivity can be directed toward the desired products. One way to achieve this is by changing donor atoms in ligands, *e.g.* nitrogen, oxygen, phosphorus, sulfur, *etc.*; and a more subtle way is to change the substituents on the ligands, thereby influencing the catalytic centre electronically and/or sterically. An additional advantage of the ligands with heterodonor sets is that the hardness/softness of the ligand can be adjusted so as to accommodate variations in the hardness/softness property of the metal ions.

Since tridentate ligands which comprise three donor groups like [O,X,O] where X = N or S have been found to form complexes with copper(II) which are active catalysts for aerial oxidation of alcohols and for oxidative C–C coupling reactions, we have extended our study of the type of ligands H_2L^S[3] and H_2L^N[4] and prepared the new ligands H_2L^P and $H_2L^{P=O}$ to investigate their coordination behaviours with transition metal ions. The ligands H_2L^P and $H_2L^{P=O}$ are abbreviated as H_2L and H_2LO in the paper, respectively. In forthcoming papers we will describe the catalytic properties of these complexes.

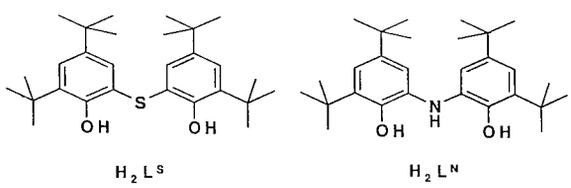

H_2L^S H_2L^N

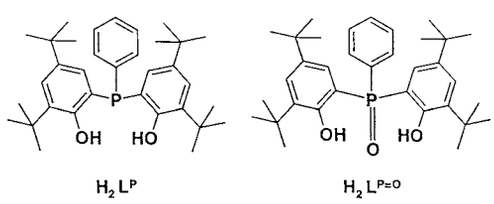

H_2L^P $H_2L^{P=O}$

Results and discussion

Synthesis and characterization of the ligands

Unsubstituted bis(*o*-hydroxyphenyl)phenylphosphine containing the donor atoms O⌒P⌒O has been prepared for the first time in 50% yield from *ortho*-bromophenol *via* reaction with n-butyllithium followed by dichlorophenylphosphine.[6] The same ligand was described as an intermediate in the synthesis of macrocyclic monophospha-crown ether ligands starting from anisole; *ortho*-lithiated anisole was treated with dichlorophenylphosphine to afford the bis adduct of methyl phenyl ether, which was subsequently demethylated with 48% HBr to yield 62% of the desired phosphine.[7] A third method in which the methoxymethyl group was used to protect the phenolic OH for the synthesis of unsubstituted bis(*o*-hydroxyphenyl)-phenylphosphine with a yield of 67% is also known.[8] On the basis of our experience in reactions with 2,4-di-*tert*-butylphenol, we realized that the first methodology, starting from *ortho*-bromophenol, can be extended to the preparation of sterically demanding phenolic derivatives with *ortho*- and

 DOI: 10.1039/b005693f

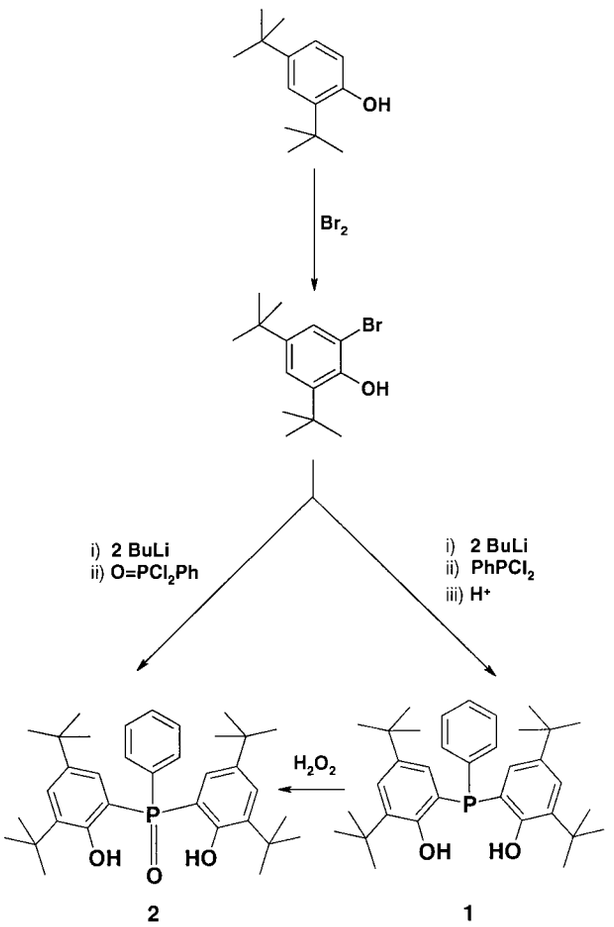

Scheme 1

para-tert-butyl substituents. So we adapted a method using 2-bromo-4,6-di-*tert*-butylphenol to our preparation of the ligand H_2L^P, **1** (Scheme 1). A very similar method has been used by us for preparation of $H_2L^{P=O}$, **2**, by using dichlorophenylphosphine oxide instead of dichlorophenylphosphine.

Ligand **2** can also be prepared by treating **1** with H_2O_2 and purified by thin layer chromatography in very good yield (95%). Ligand **2** without the *tert*-butyl groups, *i.e.* bis(*o*-hydroxyphenyl)phenylphosphine oxide, prepared in a completely different way, has been reported.[9] The ligands **1** and **2** are soluble in a range of organic solvents and stable to hydrolysis and aerial oxidation in the solid state, but **1** in solution is susceptible to aerial oxidation to **2**.

1 and **2** were fully characterized by ^{31}P, ^{1}H, ^{13}C NMR, mass and IR spectroscopy and microanalysis together with their melting point determinations. X-Ray structural data for **2** were also obtained and are reported here. The IR bands due to ν(OH), ν(C–H of t-Bu), ν(C=C), ν(P–Ph), ν(P=O) are readily identified for free **1** and **2**. ν(OH) of **1**, which occurs as a strong peak at around 3400 cm^{-1}, serves as a useful indication that complexation has occurred. There is a distinct bathochromic shift typical for phenolates on coordination to transition metal centres. For both ligands **1** and **2** the mass spectrometric parent ion peaks at $m/z = 518$ for **1** and 534 for **2** were observed, consistent with the elemental analysis. In the ^{31}P-$\{^{1}H\}$ NMR spectrum in $CDCl_3$ a singlet at δ −49.9 for **1** was observed, which is in the region expected for a trivalent phosphine.[10,11] A singlet at δ +52.6 was present in the spectrum of **2**. Thus there is a downfield shift of 102.5 ppm in the values of the ^{31}P chemical shift on oxidizing P^{III} in **1** to P^{V} in **2**.

Single crystal X-ray diffraction studies

Molecular structure of compound 2. Fig. 1 displays the structure of compound **2** in the solid state. The X-ray analysis

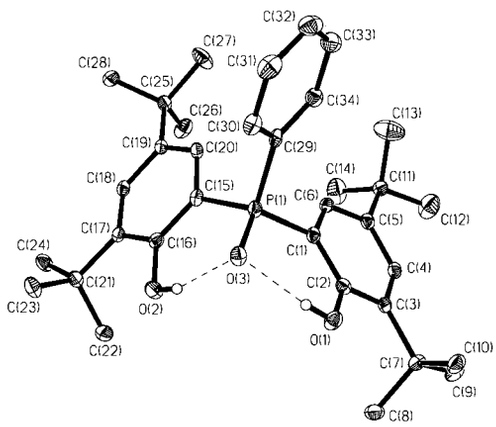

Fig. 1 An ORTEP[12] diagram of the ligand $H_2L^{P=O}$ **2**.

Table 1 Selected bond lengths (Å) and angles (°) for H_2LO, **2**

P(1)–O(3)	1.514(2)	C(16)–O(2)	1.364(3)
P(1)–C(1)	1.805(2)	C(2)–O(1)	1.360(3)
P(1)–C(29)	1.807(2)		
P(1)–C(15)	1.801(2)		
O(3)–P(1)–C(29)	110.27(11)	P(1)–C(1)–C(2)	120.5(2)
O(3)–P(1)–C(1)	110.42(10)	P(1)–C(1)–C(6)	119.7(2)
O(3)–P(1)–C(15)	110.32(10)	P(1)–C(29)–C(34)	124.6(2)
C(1)–P(1)–C(29)	109.46(11)	P(1)–C(29)–C(30)	115.9(2)
C(29)–P(1)–C(15)	109.60(11)	P(1)–C(15)–C(16)	119.1(2)
C(1)–P(1)–C(15)	106.70(11)	P(1)–C(15)–C(20)	120.2(2)

of single crystals of **2**, H_2LO, performed at 100 K, reveals strong hydrogen bonding between the phenolic hydroxyl groups and the O=P group in the solid state (O2 · · · O3 2.645 and O3 · · · O1 2.638 Å). The bond lengths and angles (Table 1) seem reasonable and do not warrant special discussion.

Molecular structure of compound 3, *trans*-(P,P)-[Ni(HL)$_2$]. A single-crystal structure analysis of green complex **3** confirms the *trans* configuration for the nickel(II) complex. An ORTEP drawing of the molecule is displayed in Fig. 2, with selected bond distances and angles provided in Table 2.

The geometry about the Ni atom is distorted square planar, consisting of a *trans* arrangement defined by P(1), P(2) and the phenoxide oxygen atoms O(2) and O(4). The deviation of the geometry around the Ni(1) from square planar is evident from the acute angles defined by the five-membered metallacycle Ni(1)P(1)C(21)C(22)O(2) for which P(1)–Ni(1)–O(2) 86.5(1)° and Ni(1)P(2)C(61)C(62)O(4) for which P(2)–Ni(1)–O(4) 87.0(1)°. Ring strain in **3** is also evidenced by angles of O(4)–Ni(1)–O(2) 172.4(1)° and P(2)–Ni(1)–P(1) 161.1(1)°. Hydrogen atoms attached to the phenol oxygens O(1) and O(3) have been detected in the Fourier difference map and strong hydrogen bonds can be envisaged between phenoxide oxygens O(4), O(2) and phenol oxygens O(1), O(3), respectively, with the contacts O(1) · · · O(4) 2.781 Å and O(3) · · · O(2) 2.715 Å. The Ni–P bond lengths av. 2.183(1) Å and av. Ni–O(phenoxide) 1.862(2) Å are consistent with other values found in the literature.[11,13,14] Axial interactions involving the nickel centre and pendant phenol groups are longer than the sum of the covalent radii[15] of the two atoms (Ni(1) · · · O(1) 3.374 and Ni(1) · · · O(3) 3.480 Å), which is in accord with the diamagnetism of **3** both in solution and the solid state.

Molecular structure of [Co(OH$_2$)(HL)(L)]·1.25THF 4. Single crystals of brown *fac-cis*(P,P)-[Co(OH$_2$)(HL)(L)] **4** were obtained from tetrahydrofuran solution by slow evaporation. The ORTEP diagram of **4** is shown in Fig. 3, while selected bond distances and angles are summarized in Table 3.

The overall geometry around the cobalt atom Co(1) is best described as a distorted facial octahedron with two *cis* phos-

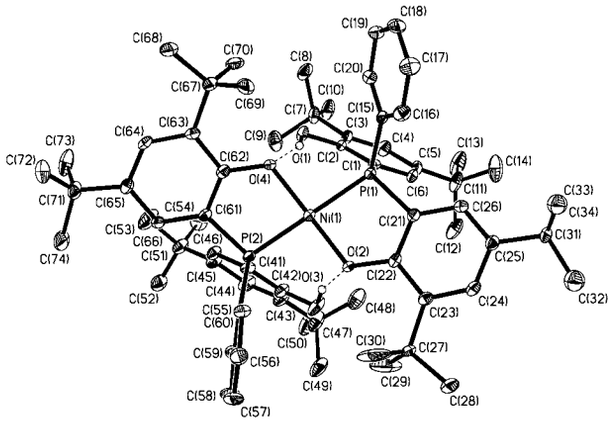

Fig. 2 Molecular structure of $[Ni^{II}(HL)_2]$ **3**.

Table 2 Selected bond distances (Å) and angles (°) for $[Ni(HL)_2]$, **3**

Ni(1)–O(4)	1.859(2)	Ni(1)–P(1)	2.186(1)
Ni(1)–O(2)	1.866(2)	Ni(1)–P(2)	2.180(1)
C(55)–P(2)–Ni(1)	117.6(1)	C(15)–P(1)–C(15)	124.2(1)
C(61)–P(2)–Ni(1)	99.4(1)	C(1)–P(1)–Ni(1)	109.1(1)
C(41)–P(2)–Ni(1)	112.0(1)	C(21)–P(1)–Ni(1)	99.0(1)
C(55)–P(2)–C(61)	110.8(2)	C(15)–P(1)–C(1)	105.7(2)
C(55)–P(2)–C(41)	108.0(2)	C(21)–P(1)–C(1)	107.9(2)
C(61)–P(2)–C(41)	108.5(2)	C(21)–P(1)–C(15)	110.1(2)
O(4)–Ni(1)–O(2)	172.4(1)	O(4)–Ni(1)–P(2)	87.0(1)
O(2)–Ni(1)–P(2)	94.3(1)	O(4)–Ni(1)–P(1)	94.7(1)
O(2)–Ni(1)–P(1)	86.5(1)	P(2)–Ni(1)–P(1)	161.1(1)

phine ligands **1**. The doubly deprotonated ligand, $[O\frown P\frown O]^{2-}$, is bound in a facial manner, the meridional mode being sterically unavailable. The second phosphine ligand is present in the monoprotonated form $[HO\frown P\frown O]^{-}$. It coordinates in a bidentate fashion with a dangling phenolic OH group, O(2), such that its P(1) donor is *cis* to the P(2) in $[OPO]^{2-}$. The sixth coordination site is occupied by a water molecule, presumably derived from moisture present in trace amounts in the solvent. A hydrogen bond is present between the dangling non-coordinated O(2) and the cobalt-bound phenolate O(4) with the O(2)···O(4) distance of 2.650 Å. The Co(1) atom is 0.137 Å out of the equatorial plane formed by the donors O(4), P(2), O(1) and O(10). All the phenyl rings attached to the P atoms are found to be planar, indicating that upon coordination the aromaticity of the phenyl rings is retained.

The cobalt–water bond, Co(1)–O(10) at 2.049(3) Å, is in the range of comparable bond lengths reported[16,17] and significantly longer than the Co–O(phenolate) bond lengths, average 1.925(2) Å. The Co(1)–P(1) bond length at 2.185(1) Å is somewhat longer than the Co(1)–P(2) bond at 2.142(1) Å, indicating that the double-phenolato anchored P donor in tridentate $[OPO]^{2-}$ is bound to the cobalt centre significantly more closely than the single-phenolato anchored P atom in bidentate $[HOPO]^{-}$ and these bond distances belong to the lower range of Co^{III}–P bond lengths known.[17] The strengthening of the Co–P bond with increased anchoring can be explained by the synergistic electronic effect ($\sigma + \pi$) as well as reduced steric effects[18] due to reorientation and bonding of the anchoring arms. The orientation of the *o*-oxyphenyl rings is coplanar or perpendicular to the equatorial plane, possibly locating the P atom in a position that favours transferring π donation from the metal to the *o*-oxyphenyl rings. Thus, the steric repulsion decreases and the π back bonding and σ bonding increases in the order of $[HOPO]^{-}$, $[OPO]^{2-}$, resulting in Co–P distances that decrease in the same order.

The distortion from octahedral geometry is mainly caused by the acute bite angles between the phenolate O atom and the P atom of the $[OPO]^{2-}$ and $[HOPO]^{-}$ ligands: P(1)–Co(1)–O(1) 86.08(8), P(2)–Co(1)–O(3) 82.07(7) and P(2)–Co(1)–O(4) 87.60(7)°. While the P(1)–Co(1)–O(3) angle is 173.56(8)°, the corresponding P(2)–Co(1)–O(10) angle at 161.90(9)° deviates remarkably from linearity.

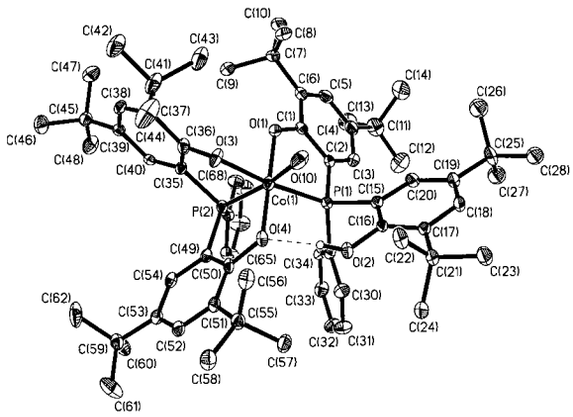

Fig. 3 Structure of the brown crystals of $[Co^{III}(OH_2)(HL)(L)]\cdot 1.25$ THF **4**. The THF molecules have been omitted for clarity.

Table 3 Selected bond lengths (Å) and angles (°) for $[Co(OH_2)(HL)(L)]\cdot 1.25$THF, **4**

Co(1)–O(1)	1.898(2)	P(1)–C(15)	1.830(4)
Co(1)–O(4)	1.922(2)	O(1)–C(1)	1.332(4)
Co(1)–O(3)	1.955(2)	O(2)–C(16)	1.378(4)
Co(1)–O(10)	2.049(3)	P(2)–C(49)	1.783(3)
Co(1)–P(2)	2.1416(10)	P(2)–C(35)	1.786(3)
Co(1)–P(1)	2.1849(11)	P(2)–C(63)	1.801(3)
P(1)–C(2)	1.789(4)	O(3)–C(36)	1.329(4)
P(1)–C(29)	1.819(3)	O(4)–C(50)	1.346(4)
O(1)–Co(1)–O(4)	178.30(10)	O(4)–Co(1)–P(1)	94.63(7)
O(1)–Co(1)–O(3)	87.91(11)	O(3)–Co(1)–P(1)	173.56(8)
O(4)–Co(1)–O(3)	91.32(10)	O(10)–Co(1)–P(1)	96.26(8)
O(1)–Co(1)–O(10)	93.82(11)	P(2)–Co(1)–P(1)	100.62(4)
O(4)–Co(1)–O(10)	84.57(11)	C(2)–P(1)–C(29)	108.9(2)
O(3)–Co(1)–O(10)	81.83(10)	C(2)–P(1)–C(15)	108.2(2)
O(1)–Co(1)–P(2)	93.79(8)	C(29)–P(1)–C(15)	103.5(2)
O(4)–Co(1)–P(2)	87.60(7)	C(2)–P(1)–Co(1)	99.49(12)
O(3)–Co(1)–P(2)	82.07(7)	C(29)–P(1)–Co(1)	121.80(11)
O(10)–Co(1)–P(2)	161.90(9)	C(15)–P(1)–Co(1)	114.35(12)
O(1)–Co(1)–P(1)	86.08(8)		

Although all the C–O bond lengths except one found in complex **4** are unremarkable (average 1.336(4) Å), the C–O bond length in the dangling phenol group is significantly longer, C(16)–O(2) 1.378(4) Å. The Co–O and Co–P bond lengths are in accord with those of a low-spin d^6 cobalt(III) complex.[17,19,20]

Molecular structure of $[RhCl(H_2L)(L)]\cdot H_2O$ 5. Orange crystals of **5**, *fac-cis*-(P,P)-$[RhCl(H_2L)(L)]\cdot H_2O$ were easily grown to suitable size from a pentane solution. The crystal structure of **5** (Fig. 4, Table 4) shows that two phosphine ligands H_2L^P are coordinated to Rh(1) *via* two phenolate, O(1) and O(2), two phosphorus P(1) and P(2) and one phenol O(4) groups, so that one of the ligands acts as a tridentate chelate and the second with a dangling phenolic OH group, O(3), is present in the protonated phenol form O(4); thus the second ligand coordinates in a bidentate fashion *via* one phosphorus P(2) and one phenol oxygen O(4). The sixth coordination site of the Rh^{III} is occupied by an axial chloride ion, Cl(1). The overall geometry around the rhodium atom is thus best described as a highly distorted facial octahedron with *cis* position of the phosphorus atoms, P(1) and P(2). The bond lengths and angles seem reasonable[17,21] and do not warrant any special discussion.

Molecular structure of $[Co_2(LO)_2(C_2H_5OH)_3]\cdot 2C_2H_5OH$ 7. A solid mixture of deep blue and colourless crystals was obtained after recrystallization. A blue crystal of complex **7** was used

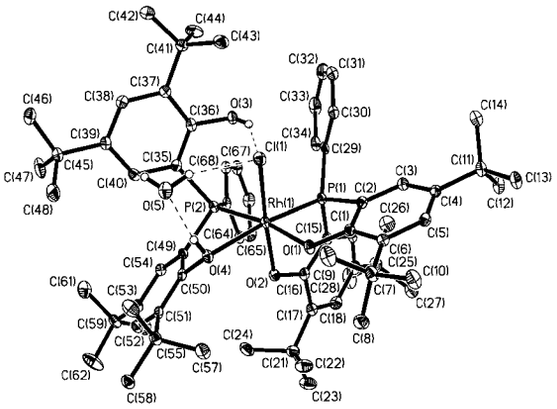

Fig. 4 An ORTEP representation of $[Rh^{III}Cl(H_2L)(L)]\cdot H_2O$ **5**. Hydrogen bonding involving the water of crystallization is also shown.

Table 4 Selected bond lengths (Å) and angles (°) for $[RhCl(H_2L)(L)]\cdot H_2O$, **5**

Rh(1)–O(2)	2.0108(14)	P(1)–C(29)	1.816(2)
Rh(1)–O(1)	2.0540(13)	P(2)–C(49)	1.816(2)
Rh(1)–P(1)	2.1814(6)	P(2)–C(63)	1.820(2)
Rh(1)–O(4)	2.2506(14)	P(2)–C(35)	1.832(2)
Rh(1)–P(2)	2.2893(6)	O(1)–C(1)	1.320(2)
Rh(1)–Cl(1)	2.3733(6)	O(2)–C(16)	1.336(2)
P(1)–C(15)	1.788(2)	O(3)–C(36)	1.390(2)
P(1)–C(2)	1.804(2)	O(4)–C(50)	1.412(2)
O(2)–Rh(1)–O(1)	87.27(5)	C(15)–P(1)–C(2)	111.20(9)
O(2)–Rh(1)–P(1)	85.88(4)	C(15)–P(1)–C(29)	111.87(10)
O(1)–Rh(1)–P(1)	83.47(4)	C(2)–P(1)–C(29)	108.40(10)
O(2)–Rh(1)–O(4)	86.69(6)	C(15)–P(1)–Rh(1)	100.21(7)
O(1)–Rh(1)–O(4)	94.12(5)	C(2)–P(1)–Rh(1)	101.20(7)
P(1)–Rh(1)–O(4)	172.29(4)	C(29)–P(1)–Rh(1)	123.25(7)
O(2)–Rh(1)–P(2)	86.74(4)	C(49)–P(2)–C(63)	106.00(9)
O(1)–Rh(1)–P(2)	170.20(4)	C(49)–P(2)–C(35)	102.20(10)
P(1)–Rh(1)–P(2)	103.82(2)	C(63)–P(2)–C(35)	109.85(9)
O(4)–Rh(1)–P(2)	77.80(4)	C(49)–P(2)–Rh(1)	98.70(7)
O(2)–Rh(1)–Cl(1)	174.29(4)	C(63)–P(2)–Rh(1)	120.09(7)
O(1)–Rh(1)–Cl(1)	87.03(4)	C(35)–P(2)–Rh(1)	116.90(6)
P(1)–Rh(1)–Cl(1)	93.42(2)	C(1)–O(1)–Rh(1)	117.72(13)
O(4)–Rh(1)–Cl(1)	93.76(4)	C(16)–O(2)–Rh(1)	117.36(13)
P(2)–Rh(1)–Cl(1)	98.92(2)	C(50)–O(4)–Rh(1)	112.69(11)

for the diffraction study. As **7** was not obtained in pure form even after several recrystallizations, spectroscopic studies could not be performed. Hence only the structure is discussed in brief here. To the best of our knowledge there are no reports involving only the ligand $H_2L^{P=O}$.

The molecular geometry and the atomic labelling scheme are shown in Fig. 5. The structure shows that a (μ-ethanol)bis(μ-phosphoryl)dicobalt(II) complex has indeed been formed in such a way that a confacial-bioctahedral geometry containing Co^{II} as central atom is present in the lattice. Ligand **2**, $H_2L^{P=O}$, is coordinated to cobalt *via* two phenolate and one P=O group so that it acts as a tridentate chelate *via* all three oxygen atoms. Three oxygen atoms (two from the phosphoryl ligands O(1) and O(4) and one from an ethanol molecule O(9)) form the bridging atoms between two cobalt centres Co(1) and Co(2). Two phenolate oxygens O(2) and O(3) belonging to the ligand $(L^{P=O})^{2-}$ containing the phosphorus atom P(1) are bonded to two different cobalt centres, to Co(1) and Co(2), respectively. The coordination of the second $(L^{P=O})^{2-}$ ligand is similar. Each of the cobalt centres is additionally bonded to an ethanol molecule. Thus the cobalt coordination geometry is distorted octahedral with six oxygen atoms. The bond lengths and angles involving the ligand $L^{P=O}$ seem reasonable, *e.g.* the average Co–O–Co angle is 92.1°. Selected bond distances and angles are listed in Table 5. The Co(1) · · · Co(2) separation is 3.081 Å. The Co–O bond lengths can clearly be divided into two groups of *ca.* 2.0–2.15 and *ca.* 2.3 Å, the latter interestingly belonging

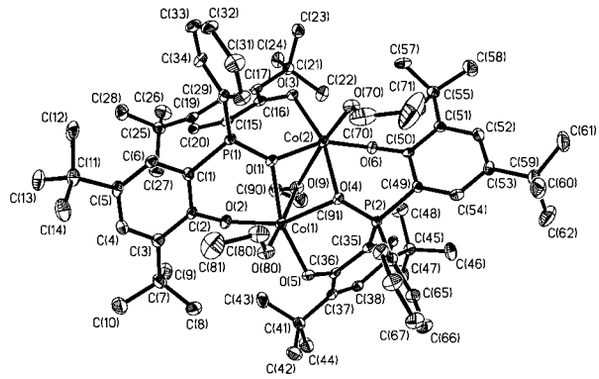

Fig. 5 A perspective view of the neutral complex $[Co^{II}_2(LO)_2(C_2H_5OH)_3]\cdot 2C_2H_5OH$ **7**. Ethanol solvent of crystallization is not shown.

Table 5 Selected bond lengths (Å) and angles (°) for $[Co^{II}_2(LO)_2(C_2H_5OH)_3]\cdot 2C_2H_5OH$, **7**

Co(1)–O(2)	1.969(3)	Co(1)–O(5)	2.023(3)
Co(1)–O(80)	2.109(3)	Co(1)–O(4)	2.115(3)
Co(1)–O(1)	2.178(3)	Co(1)–O(9)	2.332(3)
Co(2)–O(6)	1.977(3)	Co(2)–O(3)	2.015(3)
Co(2)–O(70)	2.101(3)	Co(2)–O(1)	2.120(3)
Co(2)–O(4)	2.146(3)	Co(2)–O(9)	2.369(3)
P(1)–O(1)	1.536(3)	P(1)–C(1)	1.780(4)
P(1)–C(15)	1.792(5)	P(1)–C(29)	1.803(4)
P(2)–O(4)	1.533(3)	P(2)–C(35)	1.780(4)
P(2)–C(49)	1.782(4)	P(2)–C(63)	1.795(5)
O(2)–C(2)	1.337(5)	O(3)–C(16)	1.344(5)
O(5)–C(36)	1.347(5)	O(6)–C(50)	1.328(5)
O(2)–Co(1)–O(5)	111.07(12)	O(2)–Co(1)–O(80)	95.37(13)
O(5)–Co(1)–O(80)	90.41(12)	O(2)–Co(1)–O(4)	155.56(12)
O(5)–Co(1)–O(4)	89.70(11)	O(80)–Co(1)–O(4)	97.28(13)
O(2)–Co(1)–O(1)	86.73(12)	O(5)–Co(1)–O(1)	161.23(11)
O(80)–Co(1)–O(1)	93.90(11)	O(4)–Co(1)–O(1)	71.64(11)
O(2)–Co(1)–O(9)	85.73(12)	O(5)–Co(1)–O(9)	95.76(11)
O(80)–Co(1)–O(9)	172.90(11)	O(4)–Co(1)–O(9)	79.27(11)
O(1)–Co(1)–O(9)	79.14(10)	O(6)–Co(2)–O(3)	109.70(12)
O(6)–Co(2)–O(70)	95.50(13)	O(3)–Co(2)–O(70)	93.04(13)
O(6)–Co(2)–O(1)	156.84(12)	O(3)–Co(2)–O(1)	89.34(11)
O(70)–Co(2)–O(1)	96.54(12)	O(6)–Co(2)–O(4)	87.61(11)
O(3)–Co(2)–O(4)	161.18(11)	O(70)–Co(2)–O(4)	92.52(12)
O(1)–Co(2)–O(4)	72.17(11)	O(6)–Co(2)–O(9)	85.44(11)
O(3)–Co(2)–O(9)	95.75(12)	O(70)–Co(2)–O(9)	170.28(12)
O(1)–Co(2)–O(9)	79.45(10)	O(4)–Co(2)–O(9)	77.84(11)
P(1)–O(1)–Co(2)	120.3(2)	P(1)–O(1)–Co(1)	120.6(2)
Co(2)–O(1)–Co(1)	91.56(10)	C(2)–O(2)–Co(1)	125.8(3)
C(16)–O(3)–Co(2)	121.1(2)	P(2)–O(4)–Co(1)	119.1(2)
P(2)–O(4)–Co(2)	119.6(2)	Co(1)–O(4)–Co(2)	92.61(11)
C(36)–O(5)–Co(1)	120.1(3)	C(50)–O(6)–Co(2)	124.1(3)

to the bridging oxygen atom O(9) of an ethanol molecule. The largest deviation from idealized 90° interbond angles is 21.1°, which is obtained for O(2)–Co(1)–O(5). Distortion of the cobalt centres from octahedral geometry is evident from the deviation from linearity for the O(2)–Co(1)–O(4) and O(6)–Co(2)–O(1) angles, av. 156.2°, involving the P=O and phenoxide groups. The P(1)–O(1) and P(2)–O(4) bond lengths (1.53 Å) are slightly longer than that in free $H_2L^{P=O}$, **2** (1.51 Å) (Table 1). The bond lengths are consistent with a d^7 high-spin electron configuration of the cobalt(II) centres [22] and accordingly **7** exhibits paramagnetism, detected by its ^1H NMR spectrum.

Spectroscopic and electrochemical characterization of complexes

Selected IR data for complexes **3**–**6** are given in the Experimental section. The peaks which convey most information are those due to *ν*(OH) which occur as broad peaks in the region 3143–3250 cm^{-1}. For free **1** there is a strong sharp peak at 3387 cm^{-1} present before complexation. There are strong peaks in the region 2960–2760 cm^{-1} due to the *t*-butyl groups together

with the other ν(C–H) and ν(C=C) and ν(C–O) vibrations found in the normal range for these types of linkages.[23]

The optical spectra for complexes **3**–**6** have been measured in the range 200–1000 nm in dry hexane to avoid any hydrolysis. They are dominated by charge transfer bands, as judged by the high absorption coefficients of the bands.[24] The bands at 646 nm ($\varepsilon = 520$ M^{-1} cm^{-1}) for **3**, 594(sh) for **4** and 405(640) for **5** are ascribed to the d–d transitions of the metal.

Mass spectrometry in the EI and ESI-positive mode unambiguously demonstrates the nuclearity of all the complexes examined and also provides identification of the metal centres, and, in general, the compositions are consistent with the elemental analyses. It seems that **3**–**6** are not fragile and can withstand the conditions of EIMS ionization. In the EI mass spectrum of **3** the parent ion peak is observed centred around *m*/*z* 1092 with the expected isotope distribution pattern as is confirmed by its simulation. A relatively weaker peak at *m*/*z* 517 with an abundance of ≈30% corresponding to the mono-deprotonated parent ligand $C_{34}H_{46}PO_2$ is also observed. Interestingly, the EIMS for the cobalt-containing **4** is very similar to that for **3** with the molecule ion peak centred also around *m*/*z* 1092 (100%), but with a different isotope pattern, as expected, confirming the Co : ligand ratio of 1 : 2, which is consistent with the elemental analysis.

Mass spectrometry in ESI-positive mode in CH_3OH has proved to be a very useful tool for characterization of the rhodium complex **5**. The two intense peaks centred around *m*/*z* 1173 (28%) and 1137 (100%) correspond to the molecular ion peak and the same ion that has lost one chlorine atom. Thus, that **5** contains two ligands and a chlorine atom coordinated to a rhodium atom is without doubt.

The mass spectrum in EI mode for complex **6** exhibits only a few peaks and the highest peak with an abundance of 100% is in conformity with $[RhL_2H]^+$, $C_{68}H_{91}O_4P_2Rh^+$, thus confirming the formulation as a molecule with a coordinated water molecule, which is necessary to make rhodium six-coordinated. No chlorine atom was observed in the mass spectrometry. Hence **6** is the rhodium analogue of **4** and possesses a similar structure, as elucidated by X-ray diffraction.

The chemical shifts in the ^{1}H NMR spectra of the complexes are given in the Experimental section. Owing to the overlapping of multiplets particularly in the aromatic hydrogen region (δ 5.0–8.5) full assignments were not attempted; nevertheless the spectra were still useful in verifying the similarities amongst **3**–**6**. On the other hand, ^{31}P-{^{1}H} NMR spectroscopy played a crucial role in both identifying and determining the purity of the complexes (absence of the P=O group).

The ^{31}P-{^{1}H} NMR spectra of complex **3** in the temperature range 223–323 K show two singlets, suggesting the presence of two isomers in solution. The isomerism is consistent with the two possible orientations *syn* and *anti* of the phenyl rings attached to the phosphorus atoms P(1) and P(2). Thus the solid state structure of **3** containing two equivalent phosphorus atoms as determined by X-ray diffraction differs from its solution structure. Upon coordination of **1** to the Ni an increase in chemical shift is observed from that of δ −49.9 for the "free" ligand to δ +10.2 and +6.9, as is generally seen for most phosphines due to the resulting deshielding effect.[25] For **4** and **6** singlets with consistent and noticeable shifts to lower fields on complexation to δ 56.6 and 60.9, respectively, are observed. This behaviour is comparable to that seen previously.[13] For **5** four sharp doublets showing couplings to both phosphorus and rhodium atoms, with ^1J(PRh) couplings in the range 124–126 Hz and ^2J(PP) 20 Hz are observed. These findings are consistent with two non-equivalent phosphorus donors being *cis* to one another.[8] Thus the solid state *cis*(P,P) structure of **5**, as revealed by X-ray diffraction, also prevails in solution.

Cyclic voltammetry (CV)[26] of complexes **3**–**6** was performed at ambient temperature in CH_2Cl_2 containing 0.1 M tetrabutylammonium hexafluorophosphate as supporting electrolyte at a glassy carbon working electrode at different scan rates. All redox potentials in the following are referenced in volts *versus* ferrocenium–ferrocene. Two irreversible oxidation waves are detected in the potential range +1.5 to 0.0 V at $E_1^{ox} = +0.860$ V and $E_2^{ox} = +1.20$ V for the ligand **1** in the presence of *t*-BuOK. These are assignable to phenoxyl radical formation from the phenolate ligand.

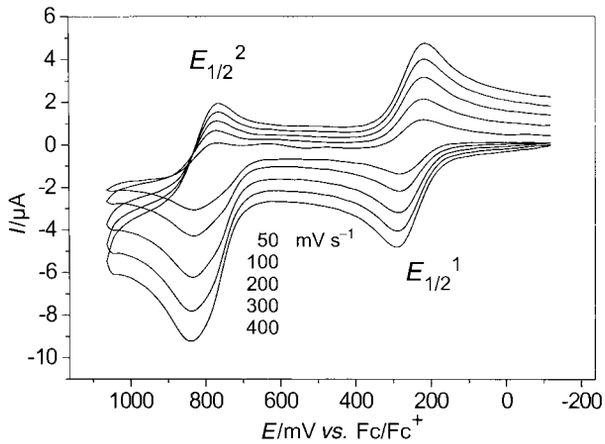

Fig. 6 Cyclic voltammograms of complex **4** in CH_2Cl_2 at different scan rates (50–400 mV s^{-1}).

Two irreversible electron-transfer waves are detected in the potential range +1.5 to 0.0 V at $E_1^{ox} = +0.386$ V and $E_2^{ox} = 0.878$ V for complex **3**. Both oxidative processes can tentatively be assigned to the phenolate ligand rather than metal-centred electron-transfer waves. This assignment is supported by comparison with the CV of **4**. Two consecutive quasi-reversible steps of oxidation at $E^1_{1/2} = +0.250$ V and $E^2_{1/2} = +0.800$ V are detected for **4**, as depicted in Fig. 6. Thus the following redox scheme, involving oxidation of the ligand (phenolate/phenoxyl) in **4**, is proposed:

$$Co^{III}(OH_2)(HL)(L) \overset{E^2_{1/2}}{\rightleftharpoons} Co^{III}(OH_2)(HL)(L^{\bullet}) \overset{E^1_{1/2}}{\rightleftharpoons} Co^{III}(OH_2)(HL^{\bullet})(L^{\bullet})$$

The cyclic voltammetric behaviour of **5** shows one reversible one-electron oxidation at +0.36 V *vs.* Fc^+–Fc, tentatively assigned to the phenolate–phenoxyl radical couple. An irreversible oxidation at +1.02 V is also attributable to the ligand oxidation.

Interestingly, the CV of complex **6**, which is the rhodium analogue of **4**, is similar to that of **4** and exhibits two consecutive quasi-reversible one-electron oxidation transfer waves detectable at $E^1_{1/2} = +0.279$ V and $E^2_{1/2} = +0.836$ V *vs.* Fc^+–Fc which are assigned to phenolate/phenoxyl radical complexes.

Experimental

Reactions were carried out in dried apparatus under a dry, inert atmosphere of argon. All chemicals were of reagent grade used as received. Solvents were dried prior to use when necessary with appropriate reagents.

Infrared spectra were recorded as KBr pellets in the range 4000–400 cm^{-1} on a Perkin-Elmer 1720X FT-IR spectrometer. Cyclic voltammograms, square-wave voltammograms, and coulometric experiments were performed on EG & G equipment (potentiostat/galvanostat model 273A). Potentials were referenced *vs.* the Ag–$AgNO_3$ electrode, and ferrocene was added as internal standard. Mass spectra were obtained with either a Finnigan MAT 8200 (electron ionization, EIMS) or a MAT 95 (electrospray ESI-MS and FAB-MS) instrument, NMR spectra on a Bruker DRX 400 instrument. All ^{1}H

chemical shifts are reported in ppm relative to tetramethylsilane and ^{31}P-{^{1}H} (162 MHz) chemical shifts relative to external orthophosphoric acid (85%).

Preparations

2-Bromo-4,6-di-*tert*-butylphenol. To a solution of 461 g (2.2 mol) of 2,4-di-*tert*-butylphenol in 900 cm^3 of CCl_4 at room temperature was added very slowly dropwise 122 cm^3 of Br_2 dissolved in 200 cm^3 of CCl_4. The resulting homogeneous faint yellow solution was stirred for 24 h at 80 °C then extracted first with 10% $NaHSO_4$ (2 × 200 cm^3) then with water (4 × 400 cm^3) and the organic phase dried over anhydrous $MgSO_4$. The dry CCl_4 layer was concentrated *in vacuo* and cooled overnight at 4 °C to yield 380 g of the product (60%), mp 57–58 °C. IR (KBr disk) (cm^{-1}): 3509 sharp (strong, ν_{O-H}), 2997–2865s (sh) (*t*-butyl, ν_{C-H}). EIMS: *m*/*z* = 284 (M^+, 21) and 271 (100%). ^1H NMR ($CDCl_3$): δ 7.34–7.24 (m, 2H), 5.65 (s, 1H), 1.42 (s, 9H) and 1.29 (s, 9H). ^{13}C NMR ($CDCl_3$): δ 148.0, 143.7, 136.7, 126.3, 123.7, 111.9, 35.8, 35.6, 31.7, 31.5, 29.7 and 29.4.

Bis(3,5-di-*tert*-butyl-2-hydroxyphenyl)phenylphosphine, H_2L 1. To a solution of 2-bromo-4,6-di-*tert*-butylphenol (4.2 g, 14.7 mmol) in absolute diethyl ether (25 cm^3) at −60 °C was added dropwise within half an hour a 1.6 M solution of *n*-butyllithium (18.4 cm^3, 29.4 mmol) in hexane. The resulting pale yellow solution was stirred for 8 h, during which time it warmed to room temperature. After it was cooled again to −50 °C, $PhPCl_2$ (1 cm^3, 7.37 mmol) dissolved in 10 cm^3 of ether was added dropwise (90 min). The reaction mixture was stirred overnight at 10 °C and for 2 h at room temperature and then the suspension of LiCl was removed by filtration under argon. The solution was extracted as fast as possible with a vigorously oxygen-free 0.1 M solution of NaH_2PO_4 (2 × 20 cm^3) followed by water. The Et_2O phase was dried over anhydrous sodium sulfate (2 h) and then concentrated to a white solid. Crystallization by cooling from acetonitrile yielded analytically pure colourless crystals of H_2L. Yield: 1.53 g (40%). mp 111–112 °C (518.71 g mol^{-1}). Calc. (found) for $C_{34}H_{47}O_2P$: C, 78.73 (78.6); H, 9.13 (9.1); P, 5.97 (6.0)%. EIMS: *m*/*z* = 518 [M^+, 100%]; ^{31}P NMR ($CDCl_3$), δ −49.9 (s, 1P). ^1H NMR ($CDCl_3$): δ 7.36–7.24 (m, 7H), 6.90 (dd, ^3J(HH) = 6.6, ^4J(HH) = 2.5, 2H), 6.28 (s, *J* 8.4 Hz, 2H, OH), 1.42 (s, 9H, *t*-Bu) and 1.16 (s, 9H, *t*-Bu). ^{13}C NMR ($CDCl_3$): δ 155.7, 155.4, 142.7, 135.7, 132.9, 132.6, 128.9, 128.6, 126.4, 118.3, 35.1, 34.4, 31.4 and 29.7. IR (KBr disk) (cm^{-1}): 3492w, 3387s (ν_{OH}), 2961, 2908, 2780s (ν_{C-H}), 1578m ($\nu_{C=C}$), 1438s (ν_{P-Ph}). Cyclic voltammogram (glassy carbon, room temp., CH_2Cl_2): $E_1^{ox} \approx 860$ mV (irrev.).

Bis(3,5-di-*tert*-butyl-2-hydroxyphenyl)phenylphosphine(v) oxide, H_2LO 2. *Method A.* 100 cm^3 of *n*-butyllithium (159 mmol) (1.6 M *n*-hexane solution) were added dropwise to a solution of 2-bromo-4,6-di-*tert*-butylphenol (22.7 g, 79.5 mmol) in 200 cm^3 of diethyl ether and stirred overnight at room temperature. The resulting yellow solution cooled at 0 °C was treated dropwise with dichlorophenylphosphine oxide (5.5 cm^3) dissolved in 50 cm^3 of diethyl ether. The reaction mixture was stirred overnight at room temperature and then the suspension of lithium halide was removed by filtration. The ether phase was washed once with 30 cm^3 of 1 M NaH_2PO_4 and 200 cm^3 of water, followed by 200 cm^3 of 1 M NaH_2PO_4. The organic layer was dried over magnesium sulfate and then the solvent was distilled off under low pressure to yield 10 g (48%) of a white solid; X-ray quality crystals were obtained from a solution in ether–pentane by evaporation. mp 194–196 °C. Calc. (found) for $C_{34}H_{47}O_3P$: C, 76.4 (76.6); H, 8.9 (8.8); P, 5.8 (5.7)%. EIMS: *m*/*z* 534 [M^+, 100] and 519 ([$H_2LO - O$]$^+$, 28%). ^{31}P NMR ($CDCl_3$): δ +52.6 (s, 1P). ^1H NMR ($CDCl_3$): δ 10.62 (s, 2H, OH), 7.61–7.44 (m, 7H) and 6.85 (dd, ^3J(HH) = 14.2, ^4J(HH) = 2.4 Hz, 2H). ^{13}C NMR ($CDCl_3$): δ 160.5, 140.6, 138.2, 132.7, 131.9, 129.3, 128.6, 126.0, 110.2, 109.2, 35.4, 34.2, 31.3 and 29.5. IR (KBr disk) (cm^{-1}): 3097m (br) (ν_{O-H}), 2962–2871s (ν_{C-H}), 1590m (sh) ($\nu_{C=C}$), 1437, 1429s (ν_{P-Ph}) and 1249s (ν_{P-O}).[27]

Method B. A solution of H_2L **1** (50 mg; 0.096 mmol) in diethyl ether was treated with a solution of H_2O_2–ether (1 : 10). Preparative TLC (hexane–ethyl acetate 30 : 1 eluent) was used to obtain 49 mg (95%) of the desired product.

[$Ni^{II}(HL)_2$], 3. To degassed absolute ethanol (10 cm^3) anhydrous $NiCl_2$ (32.4 mg; 0.25 mmol) was added and the mixture stirred at room temperature for 12 h until a clear solution was obtained. On addition of H_2L (259 mg; 0.5 mmol) a brown solid formed, which was removed by filtration and washed several times with ethanol. Recrystallization of this material from diethyl ether on cooling produced yellow-green single crystals of [$Ni(HL)_2$]. Yield: 120 mg (44%). Calc. for $C_{68}H_{92}NiO_4P_2$: C, 74.65; H, 8.48; P, 5.66. Found: C, 74.8; H, 8.4; P, 5.8%. EIMS: *m*/*z* = 1092 [M^+]. ^{31}P NMR ($CDCl_3$): δ 10.2 (s, 2P) and 6.9 (s, 2P). ^1H NMR ($CDCl_3$): δ 9.12 (s, 2H, OH), 8.74 (s, 2H, OH), 7.79–6.69 (m, 18H), 1.22 (s, 36H, *t*-Bu), 1.17 (s, 36H, *t*-Bu), 1.14 (s, 36H, *t*-Bu) and 0.91 (s, 36H, *t*-Bu). IR (KBr disk) (cm^{-1}): 3180br (ν_{OH}). UV-vis in hexane: λ_{max}/nm (ε/M^{-1} cm^{-1}) 646 (520), 457 (4570), 429 (6090) and 304 (25950). Cyclic voltammetry (CH_2Cl_2): $E^1_{1/2}$ = 386, $E^2_{1/2}$ = 878 mV.

[$Co^{III}(OH_2)(HL)(L)$]·1.25THF, 4. Anhydrous $CoCl_2$ (50.1 mg; 0.386 mmol) was dissolved in degassed dry THF (15 cm^3). Addition of solid H_2L (200 mg; 0.386 mmol) yielded a blue reaction mixture, which with NEt_3 (150 μL; 1.08 mmol) changed to deep green. The resulting solution was stirred in the presence of air for 7 days and on concentration yielded a microcrystalline solid, which was collected by filtration and washed with cold ethanol. Recrystallization from THF at room temperature gave 115 mg (25%) of X-ray quality brown crystals. Calc. for $C_{68}H_{93}CoO_5P_2$·1.25 THF: C, 73.0; H, 8.60; Co, 4.90. Found: C, 73.4; H, 8.4; Co, 5.0%. EIMS: *m*/*z* = 1092 [M^+]. ^{31}P NMR ($CDCl_3$): δ 56.6 (s, 2P). ^1H NMR ($CDCl_3$): δ 7.48–6.78 (m, 18H), 4.22 (s, 1H, OH), 1.59 (s, 18H, *t*-Bu), 1.16 (s, 18H, *t*-Bu), 1.11 (s, 18H, *t*-Bu) and 1.02 (s, 18H, *t*-Bu). IR (KBr disk) (cm^{-1}): 3190br (ν_{OH}). UV-vis in hexane: λ_{max}/nm (ε/M^{-1} cm^{-1}) 594 (sh) and 446 (1100). Cyclic voltammetry (CH_2Cl_2, glassy carbon electrode, room temp.): $E^1_{1/2}$ = 250 (rev.), $E^2_{1/2}$ = 800 mV (rev.).

[$Rh^{III}Cl(H_2L)(L)$]·H_2O, 5. To a suspension of $RhCl_3$·*n*H_2O containing 37.9% Rh (68 mg; 0.25 mmol) in dry THF (10 cm^3) was added dropwise a solution of H_2L (259 mg; 0.5 mmol) in THF (5 cm^3). The resulting red solution was concentrated on a rotary evaporator (to ≈1 cm^3), after which methanol (10 cm^3) was added. The solvent was removed again *in vacuo* and the orange solid filtered off. The solid dissolved in CH_2Cl_2 was purified by preparative TLC using CH_2Cl_2–hexane (1 : 2) as eluent. X-Ray quality orange crystals were obtained by cooling from a pentane solution. Yield: 197 mg (66%). Calc. for $C_{68}H_{94}ClO_5P_2Rh$: C, 68.53; H, 7.95; Cl, 3.0; P, 5.19. Found: C, 70.89; H, 7.80; Cl, 2.5; P, 5.5%. ESI-MS: *m*/*z* = 1173 [M^+]. ^{31}P NMR ($CDCl_3$): δ 72.7 (dd, ^1J(PRh) = 126, ^2J(PP) = 20, 1P) and 32.0 (dd, ^1J(PRh) = 124, ^2J(PP) = 20 Hz, 1P). ^1H NMR ($CDCl_3$): δ 7.53–6.44 (m, 18H), 5.56 (s, 2H, OH), 4.16 (s, 2H, $2H_2O$), 1.63 (s, 9H, *t*-Bu), 1.42 (s, 9H, *t*-Bu), 1.15 (s, 9H, *t*-Bu), 1.15 (s, 18H, *t*-Bu), 1.10 (s, 9H, *t*-Bu), 0.98 (s, 9H, *t*-Bu) and 0.97 (s, 9H, *t*-Bu). IR (KBr disk) (cm^{-1}): 3250 (br, OH). UV-vis in hexane: λ_{max}/nm (ε/M^{-1} cm^{-1}) 405 (640). Cyclic voltammetry (CH_2Cl_2, glassy carbon electrode, room temp.): $E^1_{1/2}$ = 360 (rev.), $E^2 \approx 1020$ mV (irrev.).

[$Rh^{III}(HL)(L)$]·H_2O, 6. A solution of [$RhCl(H_2L)(L)$]·H_2O (150 mg; 0.126 mmol) in CH_2Cl_2–pentane (1 : 1) was stirred for 7 d at 20 °C. Using preparative thick layer chromatography

Table 6 Crystallographic data and structure refinement for complexes **2**, **3**, **4**, **5** and **7**

	2	**3**	**4**	**5**	**7**
Empirical formula	$C_{34}H_{47}O_3P$	$C_{68}H_{92}NiO_4P_2$	$C_{68}H_{93}CoO_5P_2\cdot$ 1.25THF	$C_{68}H_{92}ClO_4P_2Rh\cdot$ H_2O	$C_{74}H_{108}Co_2O_9P_2\cdot$ $3C_2H_5OH$
Formula weight	534.69	1094.07	1201.42	1191.73	1422.5
T/K	100(2)	100(2)	100(2)	100(2)	100(2)
Crystal system	Monoclinic	Triclinic	Monoclinic	Monoclinic	Triclinic
Space group	$P2_1/n$	$P\bar{1}$	$P2_1/c$	$P2_1/n$	$P\bar{1}$
a/Å; α/°	10.153(1)	13.432(1); 89.99(2)	14.428(2)	13.4953(9)	15.036(2); 99.19(2)
b/Å; β/°	21.418(3); 97.80(2)	15.174(2); 79.00(2)	17.910(3); 95.61(2)	19.8157(12); 92.23(2)	16.294(3); 102.99(2)
c/Å; γ/°	14.176(2)	17.048(2); 72.07(2)	27.350(5)	24.397(2)	18.969(3); 108.59(2)
V/Å^3; Z	3054.1(7); 4	3238.8(6); 2	7033(2); 4	6519.3(8); 4	4155.3(12); 2
μ/mm^{-1}	0.122	0.393	0.338	0.398	0.490
Reflections collected	10765	24941	36148	39050	33548
No. unique data [$I > 2\sigma(I)$]	4630/3658	10960/6917	12335/7002	14756/10344	14060/9657
Data/restraints/parameters	4630/0/349	10960/0/675	12335/33/764	14756/1/704	14060/2/847
Final $R1$, $wR2$ [$I > 2\sigma(I)$]	0.0478, 0.11	0.0589, 0.119	0.0663, 0.16	0.0378, 0.081	0.0691, 0.164
(all data)	0.0648, 0.125	0.1152, 0.141	0.1306, 0.190	0.0679, 0.089	0.1266, 0.198

with an eluent of CH_2Cl_2–hexane (1 : 2) a yellow complex with a yield of 134 mg was isolated. Square-form yellow crystals, which became dull very quickly, were obtained by crystallization from pentane. Calc. for $C_{68}H_{93}O_5P_2Rh$: C, 70.69; H, 8.11; P, 5.36. Found: C, 70.8; H, 8.1; P, 5.1%. ESI-MS: m/z = 1137 [M$^+$]. ^{31}P NMR ($CDCl_3$): δ 60.9 (dd, ^1J(PRh) = 132 Hz). ^{1}H NMR ($CDCl_3$): δ 7.33–6.76 (m, 18H), 5.76 (s, 1H, OH), 1.56 (s, 9H, *t*-Bu), 1.19 (s, 9H, *t*-Bu), 1.14 (s, 9H, *t*-Bu) and 1.10 (s, 9H, *t*-Bu). IR (KBr disk) (cm^{-1}): 3143br (OH). UV-vis in hexane: λ_{max}/nm (ε/M^{-1} cm^{-1}) 386 (2540) and 327 (11600). Cyclic voltammetry (CH_2Cl_2, glassy carbon electrode): $E^1_{1/2}$ = 279 (rev.), E^2 = 836 mV (quasi-reversible).

$[Co^{II}_2(LO)_2(C_2H_5OH)_3]\cdot 2C_2H_5OH$, 7. To a degassed suspension of the ligand H_2LO **2** (536 mg; 1 mmol) in ethanol (30 cm^3) containing Et_3N (3 cm^3), solid $Co(OAc)_2\cdot 4H_2O$ (249 mg; 1 mmol) was added. The resulting suspension was heated to reflux under argon for 3 h to yield a deep blue clear solution, which was kept overnight in a refrigerator. A mixture of the ligand and a blue solid was obtained as the microcrystalline solid product which was recrystallized from ethanol–pentane as 0.14 g of a mixture of white ligand and blue crystals of complex **7** suitable for X-ray analysis. Several attempts to obtain a pure sample proved unsuccessful. Yield: 200 mg.

X-Ray crystallography

The crystallographic data of $H_2L^{P=O}$ **2**, $[Ni^{II}(HL)_2]$ **3**, $[Co^{III}(OH_2)(HL)(L)]\cdot 1.25THF$ **4**, $[Rh^{III}Cl(H_2L)(L)]\cdot H_2O$ **5** and $[Co^{II}_2(LO)_2(C_2H_5OH)_3]\cdot 2C_2H_5OH$ **7** are summarized in Table 6. Graphite monochromated Mo-Kα X-radiation (λ = 0.71073 Å) was used throughout. X-Ray diffraction data were collected on a Siemens SMART diffractometer and corrected for Lorentz and polarization effects. The structures were solved by direct methods and subsequent Fourier-difference techniques, and refined anisotropically by full-matrix least squares on F^2 with the program SHELXTL PLUS.[28] Hydrogen atoms attached to carbon were placed at calculated positions with isotropic thermal parameters. Those bound to oxygen were located from the difference map.

CCDC reference number 186/2239.

See http://www.rsc.org/suppdata/dt/b0/b005693f/ for crystallographic files in .cif format.

Acknowledgements

We thank Degussa-Hüls (Hanau, Germany) for a postdoctoral fellowship (to R. S.), the Fonds der Chemischen Industrie and the Max-Planck-Society for support. Skilful technical assistance of André de Bache is also thankfully acknowledged.

References

1 For example: J. A. Halfen, B. A. Jazdzewski, S. Mahapatra, L. M. Berreau, E. C. Wilkinson, L. Que, Jr. and W. B. Tolman, *J. Am. Chem. Soc.*, 1997, **119**, 8217; Y. Wang and T. D. P. Stack, *J. Am. Chem. Soc.*, 1996, **118**, 13097; D. Zurita, I. Gautier-Luneau, S. Menage, J. L. Pierre and E. Saint-Aman, *J. Biol. Inorg. Chem.*, 1997, **2**, 46; E. Bill, J. Müller, T. Weyhermüller and K. Wieghardt, *Inorg. Chem.*, 1999, **38**, 5795 and references therein; M. A. Halcrow, L. M. Lindy Chia, X. Liu, E. J. L. McInnes, L. J. Yellowlees, F. E. Mabbs, I. J. Scowen, M. McPartlin and J. E. Davies, *J. Chem. Soc., Dalton Trans.*, 1999, 1753; S. Itoh, S. Takayama, R. Arakawa, A. Furuta, M. Komatsu, A. Ishida, S. Takamuku and S. Fukuzumi, *Inorg. Chem.*, 1997, **36**, 1407; K. Yamato, T. Inada, M. Doe, A. Ichimura, T. Takui, Y. Kojima, T. Kikunaga, S. Nakamura, N. Yanagihara, T. Onaka and S. Yano, *Bull. Chem. Soc. Jpn.*, 2000, **73**, 903; Y. Shimazaki, S. Huth, A. Odani and O. Yamauchi, *Angew. Chem., Int. Ed.*, 2000, **112**, 1666.

2 *Chem. Rev.*, 1996, **96**; *Metal Ions in Biological Systems*, eds. H. Sigel and A. Sigel, Marcel–Dekker, New York, 1994, vol. 30; G. T. Babcock, M. Espe, C. Hoganson, N. Lydakis-Simantiris, J. McCracken, W. Shi, S. Styring, C. Tommas and K. Warncke, *Acta Chem. Scand.*, 1997, **51**, 533; M. M. Fontecave and J. L. Pierre, *Bull. Soc. Chim. Fr.*, 1996, **133**, 653; D. P. Goldberg and S. J. Lippard, *Adv. Chem. Ser.*, 1995, **246**, 59; J. Stubbe and W. A. van der Donk, *Chem. Rev.*, 1998, **98**, 705.

3 P. Chaudhuri, M. Hess, U. Flörke and K. Wieghardt, *Angew. Chem., Int. Ed.*, 1998, **110**, 2217.

4 P. Chaudhuri, M. Hess, T. Weyhermüller and K. Wieghardt, *Angew. Chem., Int. Ed.*, 1999, **38**, 1095.

5 P. Chaudhuri, M. Hess, J. Müller, K. Hildenbrand, E. Bill, T. Weyhermüller and K. Wieghardt, *J. Am. Chem. Soc.*, 1999, **121**, 9599.

6 A. Tzschach and E. Nietschmann, *Z. Chem.*, 1980, **20**, 341.

7 A. van Zon, G. J. Torny and J. H. G. Frijns, *Recl. Trav. Chim. Pays-Bas*, 1983, **102**, 326.

8 H. Luo, I. Setyawati, S. J. Rettig and C. Orvig, *Inorg. Chem.*, 1995, **34**, 2287.

9 R. S. Tanke, E. M. Holt and R. H. Crabtree, *Inorg. Chem.*, 1991, **30**, 1714.

10 M. Hesse, H. Meier and B. Zeeh, *Spektroskopische Methoden in der Organischen Chemie*, Georg Thieme Verlag, Stuttgart, 1995.

11 J. Heinicke, M. He, A. Dal, H.-F. Klein, O. Hetche, W. Keim, U. Flörke and H.-J. Haupt, *Eur. J. Inorg. Chem.*, 2000, 431; P. Bhattacharya, M. L. Loza, J. Parr and A. M. Z. Slawin, *J. Chem. Soc., Dalton Trans.*, 1999, 2917.

12 C. K. Johnson, ORTEP II, Report ORNL-5138, Oak Ridge National Laboratory, Oak Ridge, TN, 1976.

13 J. Parr and A. M. Z. Slawin, *Inorg. Chim. Acta*, 2000, **303**, 116.

14 J. Heinicke, M. Koesling, R. Brüll, W. Keim and H. Pritzkow, *Eur. J. Inorg. Chem.*, 2000, 299.

15 F. A. Cotton and G. Wilkinson, *Advanced Inorganic Chemistry*, 5th edn., John Wiley & Sons, New York, 1988.

16 S. Alvarez and C. Lopez, *Inorg. Chim. Acta*, 1982, **64**, L99.

17 *Comprehensive Coordination Chemistry*, eds. G. Wilkinson, R. D. Gillard and J. A. McCleverty, Pergamon Press, Oxford, 1987, vol. 4.

18 W. Levason, in *The Chemistry of Organophosphorus Compounds*, ed. F. R. Hartley, Wiley-Interscience, Chichester, 1990, vol. 1, ch. 15.

19 L. Sacconi and F. Mani, *Transition Met. Chem.* (*N. Y.*), 1982, **8**, 179 and references cited therein.

20 K. Heinze, G. Huttner and O. Walter, *Eur. J. Inorg. Chem.*, 1999, 593.
21 F. H. Allen, G. Chang, K. K. Cheung, T. F. Lai, L. M. Lee and A. Pidcock, *Chem. Commun.*, 1970, 1297; A. C. Skapski and F. A. Stephens, *J. Chem. Soc.*, *Dalton Trans.*, 1973, 1789.
22 F. A. Cotton and R. H. Soderberg, *J. Am. Chem. Soc.*, 1963, **85**, 2402.
23 A. Y. Girgis and A. L. Balch, *Inorg. Chem.*, 1975, **14**, 2724; A. Ozarowski, B. R. McGarvey, A. El-Hadad, Z. Tian, D. G. Tuck, D. J. Krovich and G. C. DeFotis, *Inorg. Chem.*, 1993, **32**, 841; S. Bruni, A. Caneschi, F. Cariati, C. Delfs, A. Dei and D. Gatteschi, *J. Am. Chem. Soc.*, 1994, **116**, 1388; S. K. Larsen and C. G. Pierpont, *J. Am. Chem. Soc.*, 1988, **110**, 1827; C. L. Simpson, S. R. Boone and C. G. Pierpont, *Inorg. Chem.*, 1989, **28**, 4379.
24 A. B. P. Lever, *Inorganic Electronic Spectroscopy*, Elsevier, Amsterdam, 1984.
25 R. V. Parish, *NMR, NQR, EPR and Mössbauer Spectroscopy in Inorganic Chemistry*, 1st edn., Ellis Horwood, New York, 1990.
26 A. Sokolowski, H. Leutbecher, T. Weyhermüller, R. Schnepf, E. Bothe, E. Bill, P. Hildebrandt and K. Wieghardt, *J. Biol. Inorg. Chem.*, 1997, **2**, 444.
27 W. Kläui and K. Dehnicke, *Chem. Ber.*, 1978, **111**, 451.
28 G. M. Sheldrick, SHELXTL PLUS, program package (PC version), Siemens Analytical X-ray Instruments Inc., Madison, WI, 1990.